

ULTRAFAST VISUALIZATION OF QUASI-THREE-DIMENSIONAL ELECTRIC FIELD OF RELATIVISTIC ELECTRON BEAM

K. Kan^{1,2†}

¹National Institutes for Quantum Science and Technology (QST), Sendai, Miyagi

²SANKEN, The University of Osaka, Osaka, Japan

Abstract

EM (electromagnetic) field around a relativistically accelerated charged particle is known to be squeezed longitudinally. This behavior is called the Lorentz contraction, and no inconsistent phenomena have been found. However, an experiment has not directly confirmed the Lorentz contraction of the EM field. The first direct observation of the Lorentz contraction of the EM field was recently performed using an electron linac at the University of Osaka. The electric (Coulomb) field around a sub-picosecond electron beam with an energy of 35 MeV was measured by an electro-optic (EO) sampling method. A single-shot electric field measurement system was developed using EO sampling and an echelon mirror. A modulated laser light due to the Pockels effect was decoded into a spatio-temporal image of the electric field, and the Lorentz contraction was directly confirmed. This ultrafast measurement technique can help longitudinal diagnostics of a charged particle beam. This presentation will report ultrafast visualization of quasi-three-dimensional (transverse and longitudinal) electric fields of a relativistic electron beam and their evolutions.

INTRODUCTION

Until recently, the validity of special relativity (SR) [1] in electromagnetism has been implicitly accepted. However, this assumption was revealed to be not on a strong experimental basis; the decisive demonstration was achieved by a picture of the relativistic Coulomb field, which is generated by a highly energetic electron beam [2] based on ultrafast (sub-picosecond) diagnostics of electric fields using electro-optic (EO) sampling. Applying the electro-optic (EO) sampling to relativistic electron beams started in 2000 to estimate the pulse width of the electron beam from that of the Coulomb field [3]. However, research on the nature of the relativistic Coulomb field is hardly reported. There are still properties of SR in electromagnetism that were not dealt with by the previous work [2], such as the Coulomb field in the longitudinal direction and the magnetic field around the highly energetic electron beam.

For the detection of electric fields, EO sampling is a good candidate for ultrafast detection. Previously, THz generation using an EO crystal and laser was proposed as EO shock waves in the 1980s [4, 5]. EO sampling for the Cherenkov cone generated in an EO material was also

performed using LiTaO₃. In EO detections, a birefringence of the EO crystal is induced by an external electric field such as a THz pulse. The birefringence results in a polarization change of a probe laser pulse traveling through the crystal. Finally, polarization analysis of the probe laser pulse enables the measurement of waveforms of a THz pulse. EO sampling has been utilized not only for analysis of laser-based THz pulses [6–9] but the Coulomb fields induced by charged particles due to the pulse and spectral characteristics of lasers.

EO samplings for far-infrared-FEL pulses [10] and the Coulomb field of an electron bunch [3] were demonstrated in an FEL facility. Spectral decoding was developed for the analysis of individual electron bunches in a bunch train [11]. Development of EO temporal decoding using GaP (gallium phosphide) supporting broadband detection [12] realized a single-shot and broadband system, resulting in an observation of EO signals as short as 60 fs in rms [13, 14] where an optical cross correlator and second-harmonic generation were utilized. Spatial decoding for a laser-based THz source [6] had been applied to monitoring X-rays' timing [15], electron bunches' timing jitter related to environmental conditions [16], and spherical-wavefront Coulomb fields of plasma electron sources [17]. Photonic time-stretch EO sampling using optical fibers with adequate length supports single-shot analysis for coherent synchrotron radiation [18] and stabilization of a storage ring [19]. A study to demonstrate SR in electromagnetics was not conducted until Ref. [2].

In this study, quasi-three-dimensional electric field strength profiles around a sub-picosecond relativistic electron beam (energy of 35 MeV, generated by a photocathode-based linac) were measured by a single-shot spatio-temporal EO sampling with (110) and (100)-cut zinc telluride (ZnTe) crystals.

EXPERIMENTAL ARRANGEMENT

An electron beam was generated by a photocathode-based linac at the Research Laboratory for Quantum Beam Science, SANKEN, the University of Osaka [20, 21]. The linac was composed of a 1.6-cell S-band radio frequency (RF) gun with a copper cathode, a 2 m long traveling-wave linac, and an arc-type magnetic bunch compressor. The photocathode of the RF gun was excited using the fourth harmonic (262 nm, UV) of a picosecond laser (PULRISE VI, Time-Bandwidth) with a pulse energy of 130 μ J/pulse and a pulse width of 5 ps FWHM at 10 Hz. The bunch charge was adjusted by a neutral density filter for the picosecond laser. The electron bunches were accelerated in the

[†] kan.koichi@qst.go.jp

gun and linac using a 35-MW klystron at a repetition rate of 10 Hz. The electron bunches in the linac were accelerated to 35 MeV. The accelerated electron bunches were compressed to sub-picoseconds using a magnetic bunch compressor composed of bending magnets, quadrupole magnets, and sextupole magnets. At the exit of the bunch compressor, the electron bunch traveling through a titanium-foil window was measured in the air. A femtosecond laser (Tsunami with Spitfire, Spectra-Physics) synchronized to the electron bunch was utilized for a probe pulse. The linac and the two lasers were synchronized by a common RF at a frequency of 79.33 MHz, which corresponds to the 36th subharmonic of S-band (2.856 GHz) for the klystron.

Figure 1 shows the single-shot and spatio-temporal measurement system for THz electric fields around sub-picosecond electron beams generated by a photocathode-based linac. The electron bunch traveled along the axis of z in Fig. 1 (a). The THz electric field around the electron beam was initiated by a metallic boundary condition as a pellicle mirror with an aluminum deposition (P1, substrate of nitrocellulose membrane with a thickness of $2\ \mu\text{m}$ and deposited aluminum thickness of $>300\ \text{nm}$, fabricated from BP108, Thorlabs). The distance between the metallic boundary condition and the EO crystal was defined as d , which corresponds to the free space and elapsed time after the electron beam generates the Coulomb field. The electron beam joined together with the probe pulse on another organic beam splitter (P2, BP145B2, Thorlabs), which is transparent for THz electric fields. For the EO crystals (EOCs), ZnTe (110) (zinc telluride, thickness of 1 mm, JX Nippon Mining & Metals) and ZnTe (100) (thickness of 2 mm) were used for transverse and longitudinal electric field measurements, respectively, in this study. Polarization changes of the probe pulses were induced by the Coulomb fields of the electron beam via the Pockels effect, leading to a birefringence. The probe pulse from the femtosecond laser (800 nm, $<130\ \text{fs}$ FWHM, a repetition rate of 960 Hz, $<830\ \mu\text{J/pulse}$, Tsunami with Spitfire, Spectra-Physics) was expanded by a beam expander (BE). The wavefront of the probe pulse was tilted by a diffraction grating (GR25-0608, 600 grooves/mm, blaze wavelength of 750 nm, Thorlabs) based on the Littrow configuration for a diffraction order of +1 as an echelon mirror. To transfer the modified spatio-temporal distribution of the laser pulse on the grating in the horizontal (x) direction, the focusing point of the $4f$ -lens imaging [22, 23] was set on the EO crystal (EOC). A polarizer (Pol1) was used to purify the polarization component in the vertical (y) direction. The probe pulse was injected on the EO crystal with focusing in x direction using a cylindrical lens (CL1). The tilted probe pulse was transported by a combination of $4f$ -lens configuration (CL1 and CL2) and reduction imaging (L1/L2) on a CMOS camera (BG505LMG, bit depth of 8-12 bit, Toshiba Teli). To avoid blur from the grating to the camera in the horizontal (x) direction, *i.e.*, temporal blur, the intermediate image after the $4f$ -lens configuration was transferred to the camera using a reduction imaging using lenses (L1/L2). The tilt angle and the horizontal size of the

rectangular aperture determined the time window of 16.5 ps under the condition of the horizontal size of 10 mm. A blur in the vertical (y) direction, *i.e.*, spatial blur, can be considered from the EO crystal to the camera, however, the spatial blur was less than 1 mm according to an analysis of spatial resolution using a test target (R2L2S1P1, Thorlabs) set at the position of EOC. The magnifications of the $4f$ -lens and the reduction imaging were 1.0 and 0.30, respectively. The probe pulse with the polarization change due to the Coulomb field was separated by a beam splitter (BS2). Two paths for different phase-offset configurations with two quarter-wave plates (QWP1/QSP2) were developed. Finally, two probe pulses through each polarizer (transmission in x component, Pol2/Pol3) were captured by the camera. Thus, the tilted probe laser, polarization analysis, and imaging enabled the single-shot and spatio-temporal measurement of the THz Coulomb fields induced by an electron beam. The calibration factor of temporal information was estimated by an interferometric pattern. Figure 1 (b) shows a picture of the paths of the electron beam and laser.

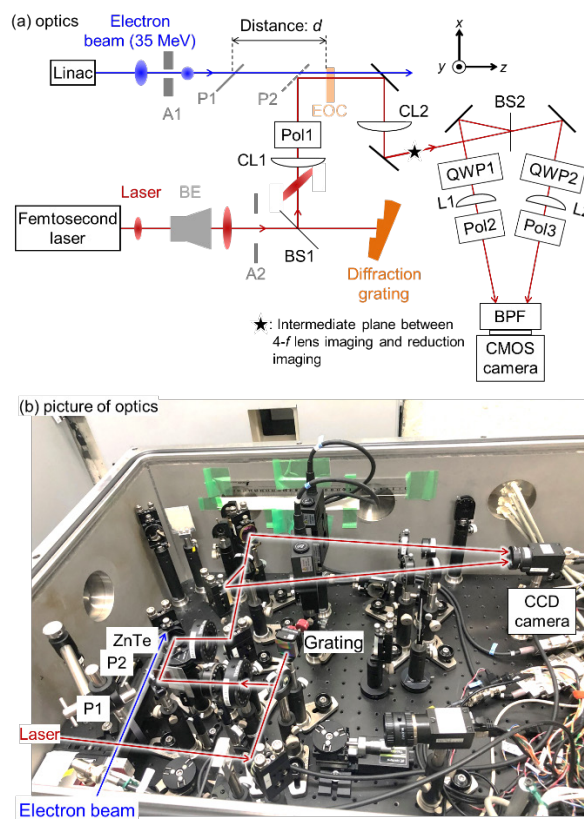


Figure 1: (a) Single-shot and spatio-temporal measurement system for THz electric fields around sub-picosecond electron beams. (b) A picture of the optics.

ANALYSIS OF ELECTRIC FIELD

To evaluate spatio-temporal profiles, the phase-offset method using a compensator [2, 23–26] was introduced. This method utilizes a light intensity, $I(\theta, \Delta)$ as a function of a phase-offset due to a QWP as a compensator, θ , and a retardation due to a birefringence of an EO crystal, Δ . The function of I corresponds to an intensity that can be applied

to an image. Images with variables of QWP and electron-beam existence are related to the retardations using signal and background images as [2, 23],

$$\frac{I(+\theta, \Delta)}{I(+\theta, 0)} - \frac{I(-\theta, \Delta)}{I(-\theta, 0)} = \frac{2 \sin \Delta}{\sin 2\theta}. \quad (1)$$

Thus, left terms are composed of four images (intensities) experimentally obtained with combinations of electron beam existence (non-zero or zero as Δ) and opposite compensators' phases (θ , 5° in this study). Furthermore, the retardation, Δ , due to transverse or longitudinal electric fields around an electron bunch in a free space, *i.e.*, E_y or E_z , are expressed with factors as,

$$\Delta_t = \frac{2\pi n_p^3 r_{41} E_y L_{110}}{\lambda} T_t = \frac{2\pi n_p^3 r_{41} E_y L_{110}}{\lambda} \frac{2}{n_{\text{THz}} + 1}, \quad (2)$$

$$\Delta_l = \frac{2\pi n_p^3 r_{41} E_y L_{110}}{\lambda} T_l = \frac{2\pi n_p^3 r_{41} E_y L_{110}}{\lambda} \frac{2}{n_{\text{THz}}(n_{\text{THz}} + 1)}, \quad (3)$$

where n_p , r_{41} , and n_{THz} denote the refractive index of 2.85 [27] at a probe wavelength of 800 nm, EO coefficient of 4 pm/V [28, 29], and refractive index of 3.18 at 1 THz [30], respectively. L_{110} and L_{100} are the thicknesses of used ZnTe (110) and ZnTe (100), respectively. Factors of T_t and T_l [9, 31] denote the Fresnel coefficients for transmission, which are the transmittances in electric fields, for the transverse and longitudinal electric fields, respectively, where an interface between the air (refractive index of 1) and the EO crystal was considered. The most effective detection can be estimated by similar approaches on refractive-index ellipsoid [31, 32]. From the ellipse, laser polarization was set [-1 1 0] and [1 0 0] for the EOC of ZnTe (110) and (100), respectively.

MEASUREMENT RESULTS

Figure 2 shows an example of the single-shot measurement acquired by the camera. Practical analysis of two functions in Eq. (1) was performed using regions of interest as cropped images, as shown in Fig. 2 (a). When the phase offset is opposite, bright and dark patterns are reversed. Figure 2 (b) and (c) show experimental results of the transverse and longitudinal THz electric fields around the relativistic electron beam, respectively. The bunch charge and electron beam size were <30 pC/pulse and <1 mm in rms, respectively. Due to a distance of $d = 45$ mm, curvatures were observed in both profiles. The transverse field was weak near the beam center ($\Delta y = 0$ mm); on the contrary, the longitudinal field was strong. And both field strengths were on the order of 1 kV/cm. These profiles are concluded in sign changes of transverse and longitudinal components in transverse and longitudinal directions, respectively.

CONCLUSIONS

Quasi-three-dimensional (transverse and longitudinal) electric fields of a relativistic electron beam with an energy of 35 MeV and a charge of <30 pC/pulse were visualized.

Single-shot spatio-temporal EO sampling was utilized for the measurement based on the phase-offset method and two-path optics. The differences in profiles between the transverse and longitudinal electric fields were clarified as sign changes according to directions. Both field strengths were on the order of 1 kV/cm.

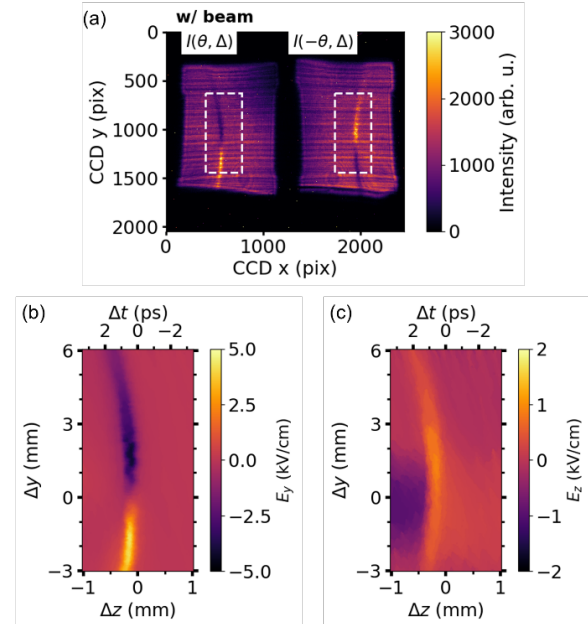


Figure 2: (a) Measurement of E_y using the camera and ZnTe (110). Left and right dashed rectangles are conditions of opposite sign for θ . The axis of time is reversed due to a beam splitter and imaging in the left and right patterns. Analysis results of (b) E_y and (c) E_z using Eq. (1)-(3). Δz and Δy denote longitudinal and transverse positions for the beam center, respectively. These examples were performed at $d = 45$ mm.

ACKNOWLEDGEMENTS

This work was supported by JSPS KAKENHI Grant Numbers: JP23K11702, JP23H00281, JP20H02206, JP23K13080, JP24H00317, and JP24H02232. This work was also supported by AutoRace (JKA, 2022M-225). The study used the 40-MeV S-band Laser Photocathode RF electron Linac facility provided by the Research Laboratory for Quantum Beam Science of SANKEN, the University of Osaka.

REFERENCES

- [1] A. Einstein, "Zur Elektrodynamik bewegter Körper," *Ann. Phys.*, vol. 322, no. 10, pp. 891–921, Jan. 1905. doi:10.1002/andp.19053221004
- [2] M. Ota *et al.*, "Ultrafast visualization of an electric field under the Lorentz transformation," *Nat. Phys.*, vol. 18, no. 12, pp. 1436–1440, Oct. 2022. doi:10.1038/s41567-022-01767-w
- [3] X. Yan *et al.*, "Subpicosecond Electro-optic Measurement of Relativistic Electron Pulses," *Phys. Rev. Lett.*, vol. 85, no. 16, pp. 3404–3407, Oct. 2000. doi:10.1103/physrevlett.85.3404

- [4] D. H. Auston, "Subpicosecond electro-optic shock waves," *Appl. Phys. Lett.*, vol. 43, no. 8, pp. 713–715, Oct. 1983. doi:10.1063/1.94486
- [5] D. H. Auston, K. P. Cheung, J. A. Valdmanis, and D. A. Kleinman, "Cherenkov Radiation from Femtosecond Optical Pulses in Electro-Optic Media," *Phys. Rev. Lett.*, vol. 53, no. 16, pp. 1555–1558, Oct. 1984. doi:10.1103/physrevlett.53.1555
- [6] J. Shan *et al.*, "Single-shot measurement of terahertz electromagnetic pulses by use of electro-optic sampling," *Opt. Lett.*, vol. 25, no. 6, p. 426, Mar. 2000. doi:10.1364/ol.25.000426
- [7] S. Kono, M. Tani, and K. Sakai, "Ultrabroadband photoconductive detection: Comparison with free-space electro-optic sampling," *Appl. Phys. Lett.*, vol. 79, no. 7, pp. 898–900, Aug. 2001. doi:10.1063/1.1394719
- [8] M. Nagai, E. Matsubara, and M. Ashida, "High-efficiency terahertz pulse generation via optical rectification by suppressing stimulated Raman scattering process," *Opt. Express*, vol. 20, no. 6, p. 6509, Mar. 2012. doi:10.1364/oe.20.006509
- [9] Y. Minami, T. Kurihara, K. Yamaguchi, M. Nakajima, and T. Suemoto, "Longitudinal terahertz wave generation from an air plasma filament induced by a femtosecond laser," *Appl. Phys. Lett.*, vol. 102, no. 15, p. 151106, Apr. 2013. doi:10.1063/1.4802482
- [10] G. M. H. Knippels *et al.*, "Generation and Complete Electric-Field Characterization of Intense Ultrashort Tunable Far-Infrared Laser Pulses," *Phys. Rev. Lett.*, vol. 83, no. 8, pp. 1578–1581, Aug. 1999. doi:10.1103/physrevlett.83.1578
- [11] I. Wilke, A. M. MacLeod, W. A. Gillespie, G. Berden, G. M. H. Knippels, and A. F. G. van der Meer, "Single-Shot Electron-Beam Bunch Length Measurements," *Phys. Rev. Lett.*, vol. 88, no. 12, p. 124801, Mar. 2002. doi:10.1103/physrevlett.88.124801
- [12] S. Casalbuoni, H. Schlarb, B. Schmidt, P. Schmüser, B. Steffen, and A. Winter, "Numerical studies on the electro-optic detection of femtosecond electron bunches," *Phys. Rev. Spec. Top. Accel Beams*, vol. 11, no. 7, p. 072802, Jul. 2008. doi:10.1103/physrevstab.11.072802
- [13] G. Berden *et al.*, "Benchmarking of Electro-Optic Monitors for Femtosecond Electron Bunches," *Phys. Rev. Lett.*, vol. 99, no. 16, p. 164801, Oct. 2007. doi:10.1103/physrevlett.99.164801
- [14] B. Steffen *et al.*, "Electro-optic time profile monitors for femtosecond electron bunches at the soft x-ray free-electron laser FLASH," *Phys. Rev. Spec. Top. Accel Beams*, vol. 12, no. 3, p. 032802, Mar. 2009. doi:10.1103/physrevstab.12.032802
- [15] A. L. Cavalieri *et al.*, "Clocking Femtosecond X Rays," *Phys. Rev. Lett.*, vol. 94, p. 114801, 2005.
- [16] W. Wang *et al.*, "Temporal profile monitor based on electro-optic spatial decoding for low-energy bunches," *Phys. Rev. Accel. Beams*, vol. 20, no. 11, p. 112801, Nov. 2017. doi:10.1103/physrevaccelbeams.20.112801
- [17] K. Huang *et al.*, "Electro-optic spatial decoding on the spherical-wavefront Coulomb fields of plasma electron sources," *Scientific Reports*, vol. 8, no. 1, p. 2938, Feb. 2018. doi:10.1038/s41598-018-21242-y
- [18] C. Evain *et al.*, "Direct Observation of Spatiotemporal Dynamics of Short Electron Bunches in Storage Rings," *Phys. Rev. Lett.*, vol. 118, no. 5, p. 054801, Feb. 2017. doi:10.1103/physrevlett.118.054801
- [19] C. Evain *et al.*, "Stable coherent terahertz synchrotron radiation from controlled relativistic electron bunches," *Nat. Phys.*, vol. 15, no. 7, pp. 635–639, Apr. 2019. doi:10.1038/s41567-019-0488-6
- [20] I. Nozawa *et al.*, "Measurement of <20 fs bunch length using coherent transition radiation," *Phys. Rev. Spec. Top. Accel Beams*, vol. 17, no. 7, p. 072803, Jul. 2014. doi:10.1103/physrevstab.17.072803
- [21] K. Kan *et al.*, "Time-domain measurement of coherent transition radiation using a photoconductive antenna with micro-structured electrodes," *AIP Advances*, vol. 11, no. 12, p. 125319, Dec. 2021. doi:10.1063/5.0067586
- [22] H. Hirori, A. Doi, F. Blanchard, and K. Tanaka, "Erratum: 'Single-cycle terahertz pulses with amplitudes exceeding 1 MV/cm generated by optical rectification in LiNbO₃' [*Appl. Phys. Lett.* 98, 091106 (2011)]," *Appl. Phys. Lett.*, vol. 103, no. 25, p. 259901, Dec. 2013. doi:10.1063/1.4854095
- [23] G. Asai, D. Hata, S. Harada, T. Kasai, Y. Arashida, and I. Katayama, "High-throughput terahertz spectral line imaging using an echelon mirror," *Optics Express*, vol. 29, no. 3, p. 3515, Jan. 2021. doi:10.1364/oe.413802
- [24] Z. Jiang, F. G. Sun, Q. Chen, and X.-C. Zhang, "Electro-optic sampling near zero optical transmission point," *Appl. Phys. Lett.*, vol. 74, no. 9, pp. 1191–1193, Mar. 1999. doi:10.1063/1.123495
- [25] C. C. Montarou and T. K. Gaylord, "Two-wave-plate compensator method for single-point retardation measurements," *Appl. Opt.*, vol. 43, no. 36, p. 6580, Dec. 2004. doi:10.1364/ao.43.006580
- [26] F. D. J. Brunner, J. A. Johnson, S. Grübel, A. Ferrer, S. L. Johnson, and T. Feurer, "Distortion-free enhancement of terahertz signals measured by electro-optic sampling I Theory," *Journal of the Optical Society of America B*, vol. 31, no. 4, p. 904, Mar. 2014. doi:10.1364/josab.31.000904
- [27] D. T. F. Marple, "Refractive Index of ZnSe, ZnTe, and CdTe," *J. Appl. Phys.*, vol. 35, no. 3, pp. 539–542, Mar. 1964. doi:10.1063/1.1713411
- [28] Q. Wu and X.-C. Zhang, "Ultrafast electro-optic field sensors," *Appl. Phys. Lett.*, vol. 68, no. 12, pp. 1604–1606, Mar. 1996. doi:10.1063/1.115665
- [29] J. Hebling, A. G. Stepanov, G. Almási, B. Bartal, and J. Kuhl, "Tunable THz pulse generation by optical rectification of ultrashort laser pulses with tilted pulse fronts," *Appl. Phys. B: Lasers Opt.*, vol. 78, no. 5, pp. 593–599, Mar. 2004. doi:10.1007/s00340-004-1469-7
- [30] G. Gallot, J. Zhang, R. W. McGowan, T.-I. Jeon, and D. Grischkowsky, "Measurements of the THz absorption and dispersion of ZnTe and their relevance to the electro-optic detection of THz radiation," *Appl. Phys. Lett.*, vol. 74, no. 23, pp. 3450–3452, Jun. 1999. doi:10.1063/1.124124
- [31] M. J. Cliffe, A. Rodak, D. M. Graham, and S. P. Jamison, "Generation of longitudinally polarized terahertz pulses with field amplitudes exceeding 2 kV/cm," *Appl. Phys. Lett.*, vol. 105, no. 19, p. 191112, Nov. 2014. doi:10.1063/1.4901904
- [32] Q. Chen, M. Tani, Z. Jiang, and X.-C. Zhang, "Electro-optic transceivers for terahertz-wave applications," *Journal of the Optical Society of America B*, vol. 18, no. 6, p. 823, Jun. 2001. doi:10.1364/josab.18.000823